Constructing and Characterizing TiAlN Thin Film by DC. Pulsed Magnetron Sputtering at Different Nitrogen/Argon Gas Ratios

M. Raaif

Physics Department, Faculty of Science, Sohag University, 82524-Sohag, Egypt

mraaif@daad-alumini.de

Abstract

In this survey, the magnetron sputtering with Dc. Pulsed mode was embroiled to deposit TiAlN thin film on AISI 316 as a substrate. All the plasma magnetron parameters were fixed excluding the nitrogen gas ratio which was varied from 10% to 50% with step interval of 10% with respect to argon. The structure, mechanical, tribological and electrochemical peculiarities of TiAlN films were studied. The TiAlN deposition rate is decreased in regard with increasing the nitrogen gas ratio where, the film thickness recorded a maximum value of 3 μm at nitrogen gas ratio of 10 %. X-ray configurations demonstrated the formation of solid solution phase of TiAlN with different orientations. The TiAlN coating has (111) preferred orientation at 10 and 20% nitrogen gas ratios while has (200) preferred orientation at 30-50% nitrogen gas ratios. The crystallite size is decreased with increasing the N_2 gas ratio. The results depicted that, the microhardness of TiAlN film is increased with decreasing the N_2 gas ratio and recorded a maximum value of approximately 850 HV0.015 at 10% N_2. Additionally, the tribological properties of the coated AISI 316 with TiAlN are enhanced compared with the uncoated sample. The wear volume loss of the coated sample at 10% N_2 has a value of nearly $9X10^4$ μm^3 which is low compared with the substrate that has a value of $4.5X10^6$ μm^3. The corrosion resistance of all TiAlN coatings was better than the uncoated sample. It was demonstrated; the change in nitrogen gas ratio regulated the physico-chemical features of the TiAlN coatings.

Keywords:

TiAlN thin film; Dc. Pulsed magnetron sputtering; nitrogen gas ratio; microhardness; wear rate; surface roughness; corrosion resistance

Date of Publication: 30-08-2018

DOI: 10.24297/jap.v14i2.7542

ISSN: 2347-3487

Volume: 14 Issue: 2

Journal: Journal of Advances in Physics

Website: https://cirworld.com

1. Introduction

TiAlN Coatings prepared by physical vapor deposition (PVD) were utilized in considerable industrial applications owed to respectable tribological characteristics, mechanical, anti-corrosion and high oxidation resistance [1]. TiAlN is synthesized by a variety of PVD techniques as magnetron sputtering and cathodic arc evaporation [2, 3]. The binary transition metal nitride depositions such as TiC, TiN and ZrN were extensively employed as protective layer for wear and cutting tools owed to their superior mechanical and tribological properties. Supplementary, the combination of Al in TiN and ZrN enhances the mechanical and thermal stability of the coating [4]. Nitride coatings were constructed by Dc reactive magnetron sputtering of metallic target with governing nitrogen gas atmosphere. Moreover, these coatings can be fabricated by sputtering of nitride target using direct rf (radio frequency; commonly 13.56 MHz). Though, both of these methods are problematic. Films of high-quality can be invented by rf sputtering. However, the deposition rates are very low. Moreover, the encasement of the target by reactive gas product is considered as a disturbance accompanying with the reactive magnetron sputtering and is mentioned as target poisoning [5]. The poisoned layers charged up until breakdown happens in the form of an arc. Moreover, the damaged zone on the target is accountable as a source of additional arc discharges, resulting in an increasing in the frequency of arcing. Arc demeanor avoids steady operation of the process by instigating quick vacillations in the deposition parameters. Arc occasions throughout reactive sputtering are considered as a weighty problem, because the Arc perturbs the structure, composition and properties of the growing film. The latterly progressed pulsed magnetron sputtering (PMS) defeats several problems which are faced with operating in the reactive sputtering mode. It was found; pulsed the magnetron discharge in the moderate frequency (10~200 kHz) in the deposition of insulating films can significantly diminish the establishment of arcs and accordingly minimize the number of defects in the producing film [6, 7]. Furthermore, deposition rates are enhanced by using pulsed reactive sputtering. The PMS process, therefore, permits the formation of high rate deposition of defect-free ceramic films. It was known; the physico-chemical properties of growth films by pulsed magnetron sputtering rely stalwartly on the processing conditions and parameters as gas ratio, pressure, temperature and applied bias voltage. For example, gas ratio affected the sputtered species energy from the target up to the substrate therefore modulate the film properties. This work was focused on enhancing the physico-chemical properties of AISI 316 material. This was achieved by depositing of TiAlN on the surface of AISI 316 employing Dc-pulsed magnetron sputtering at various nitrogen gas ratios. The structural, tribo-mechanical and electro-chemical properties of the involved samples have been evaluated. These surface features are the main factors that legalize the in-service performance of the coated AISI 316 for many manufacturing applications.

2. Experimental Work

2.1 Sample Preparation

TiAlN thin films were coated using Dc. Pulsed magnetron sputtering technique. The films were grown on AISI 316 substrates from highly pure disk shape of Ti-Al alloy (50-50%) with purity of 99.99% and diameter of 2 inches and thickness of 3 mm. The substrate chemical composition in wt% is: 0.024 C, 1.35Mn, 16.87 Cr, 10.05 Ni, 2.06 Mo, 0.031 P, 0.029 S and Fe balance. All specimens were cut into 10 mm x 10 mm x 1 mm then were polished employing silicon papers (600 to 4000 grit). After that the substrates were washed ultrasonically using acetone. The diagram of Dc pulsed magnetron sputtering scheme can be found somewhere else [8]. Briefly, the system is involved stainless steel chamber that has a diameter of 30 cm. The chamber was evacuated by turbo and rotary pumps to realize a base pressure of $6x10^{-6}$ mbar. Argon (Ar) and nitrogen (N_2) gases were incorporated into the chamber to establish a total working gas pressure of $5x10^{-3}$ mbar. The Dc. Pulsed power supply model: Pinnacle Plus pulsed is conducted to generate the discharge. The TiAlN coatings were prepared at plasma magnetron power of 150 W and the N_2 gas ratio was changed from 10:50 % with respect to argon. A Powerful magnet is used to ionize the Ti-Al target material and encourage it to stabilize on the substrate in the form of thin film. The AISI 316 substrates were secured on a sample holder at distance of 5 cm from the target. The deposition parameters for TiAlN layers were scheduled in table (1).

2.2 Sample Testing and Characterization

Different techniques were conducted to test and characterize the involved samples. X-ray diffraction (XRD) using Philips-PW1710 diffractometer with Cu Kα radiation of λ= 1.541838 Å was used to identify the phase constitution. The XRD scan was engaged between 30° and 90°, with step of 0.02° and rate of 1°/min. The TiAlN surface morphologies were investigated by Quanta 250 FEG scanning electron microscope (SEM).

Vickers microhardness was accomplished using Leitz Durimet microhardness at applied load of 15 gmf. The tests were run in regard with ASTM E384-11 [9]. The wear and friction tests were implemented regarding to ASTM G 133-10 at room temperature using an oscillating ball-on-disk type tribometer without lubrication. The 3 mm aluminum oxide ball moves at a mean sliding speed of 30 mm/s with a normal load of 2N has been engaged in this work. The surface roughness inspection of the samples was executed using a Form Talysurf 50 profilemeter.

The electrochemical investigations were achieved in Ringer's solution by Gill AC instrument using potentiodynamic technique at temperature of 25 ±3ºC. The operative corrosive area of the investigated samples was fixed at 0.36 cm^2. The corrosion curve (potential–current) was plotted with potential scan rate of 150 mV/min using ACM program version 5.

Table 1: operating parameters of TiAlN coatings.

Parameters	Values
Base pressure (mbar)	**$6X10^{-6}$**
Working pressure (mbar)	**$5X10^{-3}$**
N_2 Gas Ratio (%)	**10, 20, 30, 40 and 50**
Plasma-processing power (watt)	**150**
Pulse frequency (KHz)	**150**
Reverse time (µsec)	**2**
Deposition time (min)	**90**
Target to Substrate distance (cm)	**5**

3. Results and Discussion

3.1 Film Thickness and Deposition Rate

Figure 1 demonstrated the variation of TiAlN film thickness and the deposition rate as a function of N_2 gas ratio. It was observed; the film thickness decreased from 3 µm to 0.9 µm with increasing N_2 gas ratio from 10 % to 50 %. Moreover, the deposition rate is decreased from 33nm/min to 10nm/min with increasing N_2 gas ratio. The reduction in film thickness and deposition rate are logically acceptable and attributed to the target poisoning effects due to the formation of AlN and TiN hard sputtered species which in turn reduce the sputtering rate as compared to those deposited with lower nitrogen gas ratios [10, 11]. Alternatively, the increase in the nitrogen content will ordinarily decrease the argon gas content in the plasma chamber then decreasing the sputtering yield.

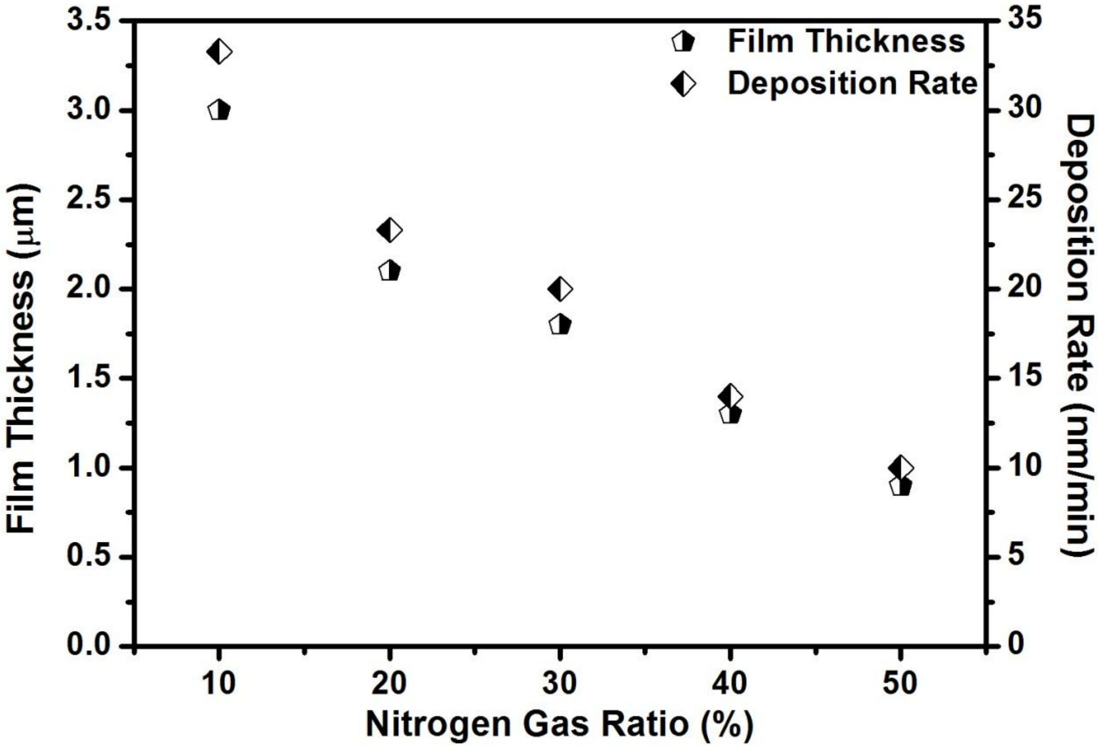

Fig. 1: TiAlN film thickness and rate of deposition variations with different nitrogen gas percentage with respect to argon

3.2 Microstructure Analysis

Figure 2 displays the surface micrographs of TiAlN thin films prepared at 80% Ar and 20 % N_2. Cauliflower-like structure with well-defined and uniformly distributed grains over the whole surface was observed in the sample morphology. This structure is categorized as densely packed structure and is formed due to the reaction between titanium and nitrogen.

Figure 3 displays the phase configuration of the investigated samples as distinguished by XRD analysis. The XRD spectra of AISI 316 substrate endorsed the presence of austenitic phases, while the spectra of the coated substrates with TiAlN designated the existence of TiAlN solid solution phase (FCC structure) with different orientations. The patterns revealed peaks at diffractive angles of 37^o, 44.18^o, 62.9^o, 75.3 and 79.42^o correspond to solid solution phases of TiAlN (111), (200), (220), (311) and (222) planes, respectively. The TiAlN (311) and TiAlN (222) solid solution phase appears at samples deposited at low nitrogen gas ratios of 10%, 20% and 30% where the sputtered species have high enough energy to form these orientations which need for relatively high energy compared with other orientations. It was witnessed; the intensity of AISI austenitic phases is decreased with increasing the film thickness. Moreover, the intensity of TiAlN solid solution phases is increased with increasing the film thickness. Further, XRD spectra for TiAlN solid solution phases displayed peak shifts of the Bragg reflections towards high angles comparing to the standard TiN diffraction pattern. The radius of Al atom is 0.1440 nm which is lower than the Ti atom radius that is equal to 0.1461 nm. This mean, the titanium atoms in TiN lattice were subrogated by aluminum atoms [12, 13].

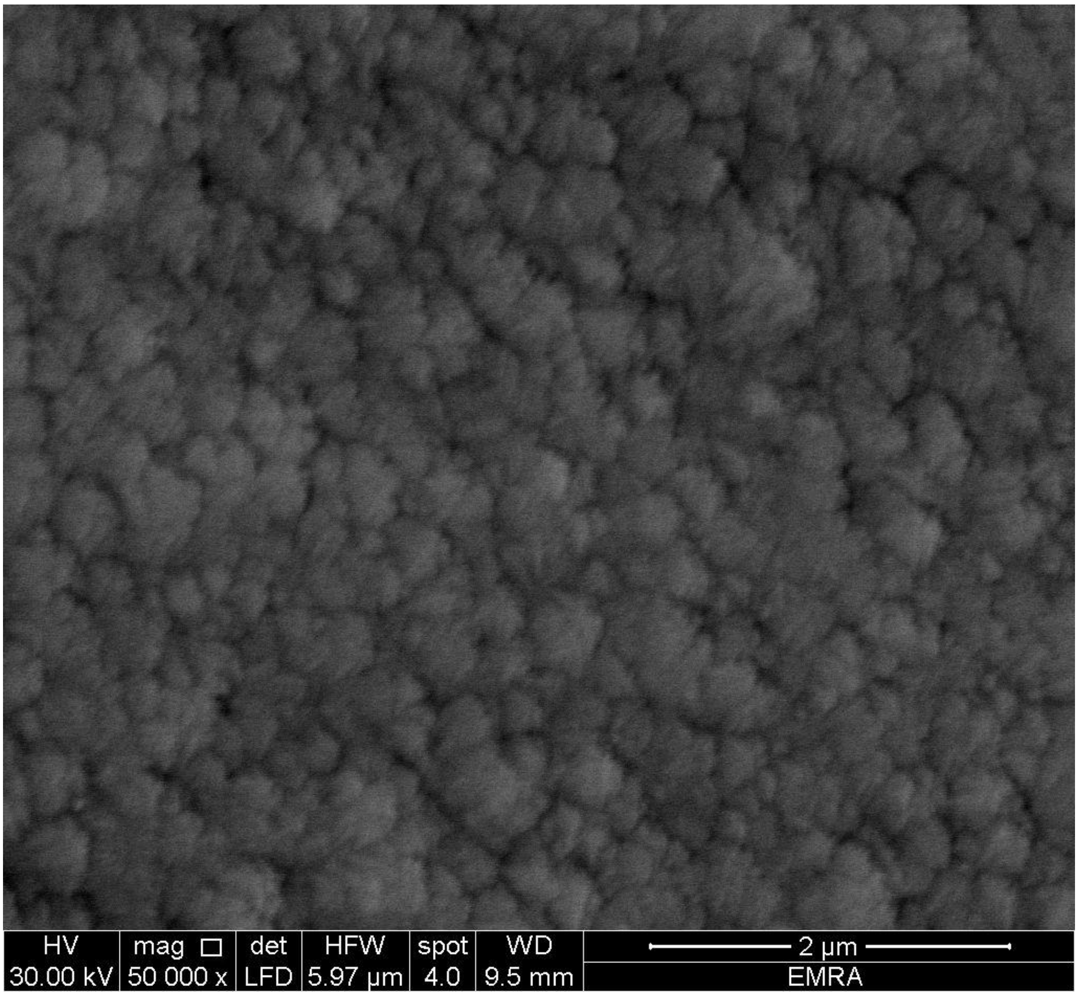

Fig. 2: FE-SEM micrographs of TiAlN film deposited at pulsed plasma power of 150W and nitrogen gas percentage of 20 %.

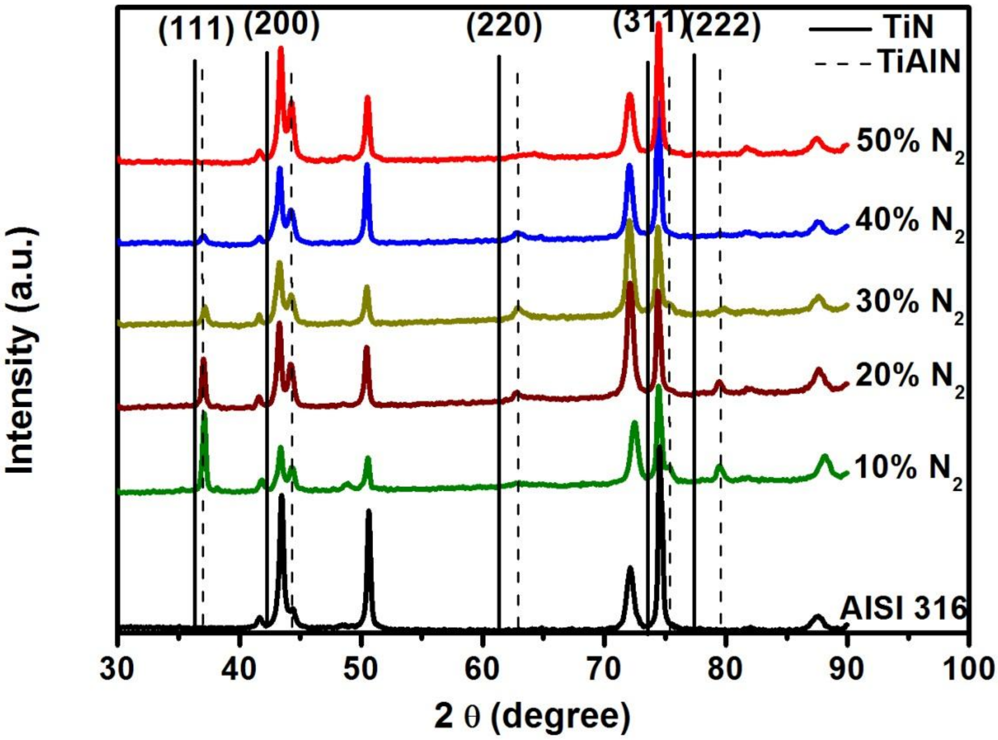

Fig. 3: XRD of AISI 316 and coated substrates with TiAlN at different nitrogen gas percentage with respect to argon

Figure 4 illustrates the estimated texture coefficient of TiAlN (111) and (200) planes as a function of nitrogen gas ratio. The results of Tc confirmed that, all prepared samples at high nitrogen gas ratio have preferred orientation along (200) direction. However, at low nitrogen gas ratio have preferred orientation along (111) direction. The amendment in preferred orientation is qualified to the decrease in high-energy ion bombardment with increasing the nitrogen gas ratio. It was mentioned; the plan (111) has respectable mechanical properties comparing with plan (200) [14].

Figure 5 illustrates the change in crystallite size of TiAlN coatings with nitrogen gas ratio. It was observed; the crystallite size of TiAlN is decreased as the nitrogen gas ratio increased. The decrease in the crystallite size is accredited to the decreased in adatoms mobility at higher nitrogen gas ratio. The transformation from metallic target to poisoning target mode due to the formation of hard sputtered species of AlN and TiN is accountable for decreasing the energy of the adatoms mobility [10, 11].

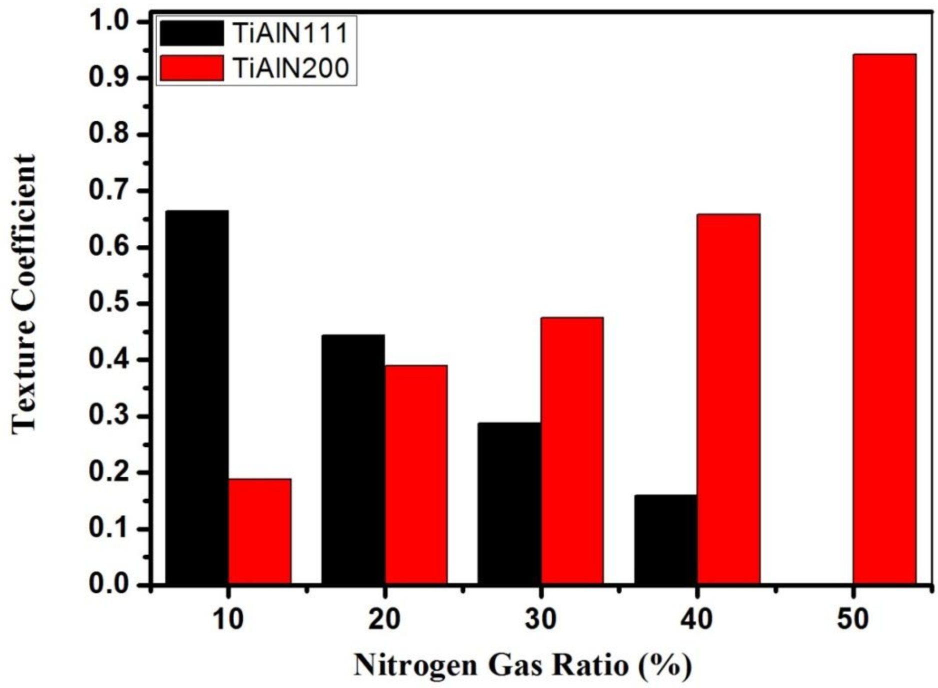

Fig. 4: Texture coefficient of TiAlN in (111) and (200) directions as a function of nitrogen gas percentage with respect to argon.

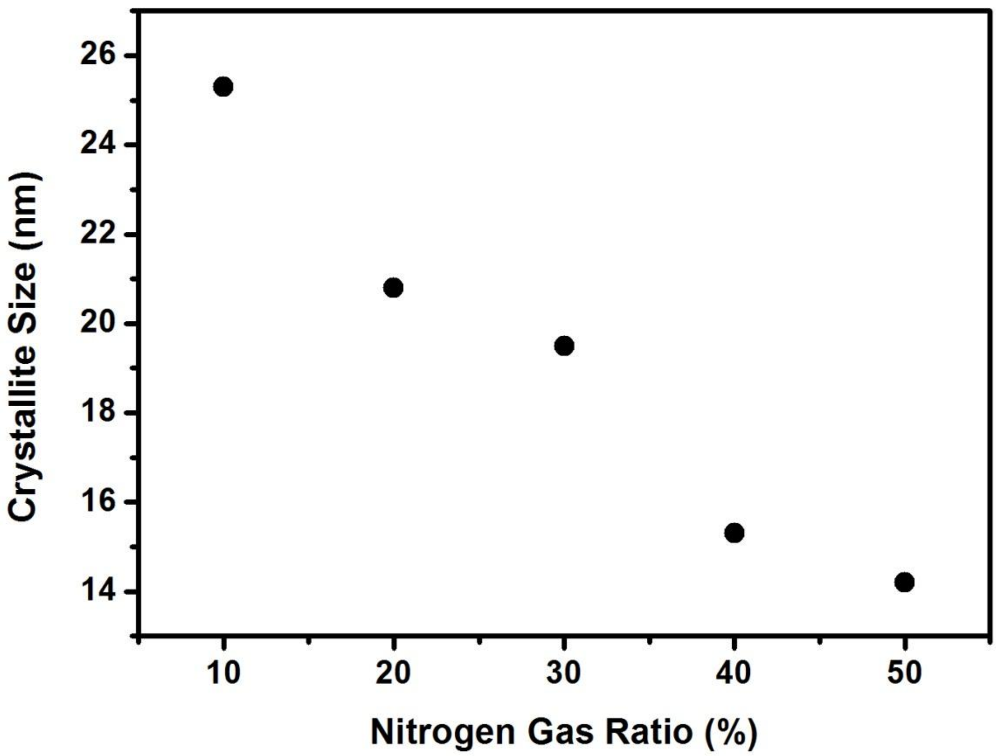

Fig. 5: Crystallite size of TiAlN films as a function of nitrogen gas percentage with respect to argon

3.3 Mechanical and Tribological Properties

3.3.1 Surface Microhardness

Figure 6 elucidates the microhardness values of the involved samples. It was perceived; the Microhardness decreased with increasing nitrogen gas ratio. The microhardness recorded 150 HV0.15 for the uncoated substrate, while recorded a maximum value of 820 HV 0.015 for the sample that was coated at 10% nitrogen gas ratio. That represents a nearly 5-fold increase in microhardness compared with AISI 316 substrate. It should be mentioned; the hardness of TiAlN thin film recorded a value greater than the obtained value in this work using nanoindentation technique. In this regard, the measured Vickers's microhardness is accountable as a compound hardness resulted from the contribution of hard TiAlN thin film and soft AISI substrate. The enhancement in hardness is endorsed to the formation of super-hard coating of TiAlN solid solution phase with preferred orientation of (111) [15]. The decreased in microhardness with increasing nitrogen gas ratio is credited to the decrease in the intensity of TiAlN (111) phase orientation and the transformation to TiAlN (200) orientation. Otherwise, the increase in the nitrogen gas ratio decreased the film thickness thus increasing the effect of low hardness substrate on the total film hardness [8].

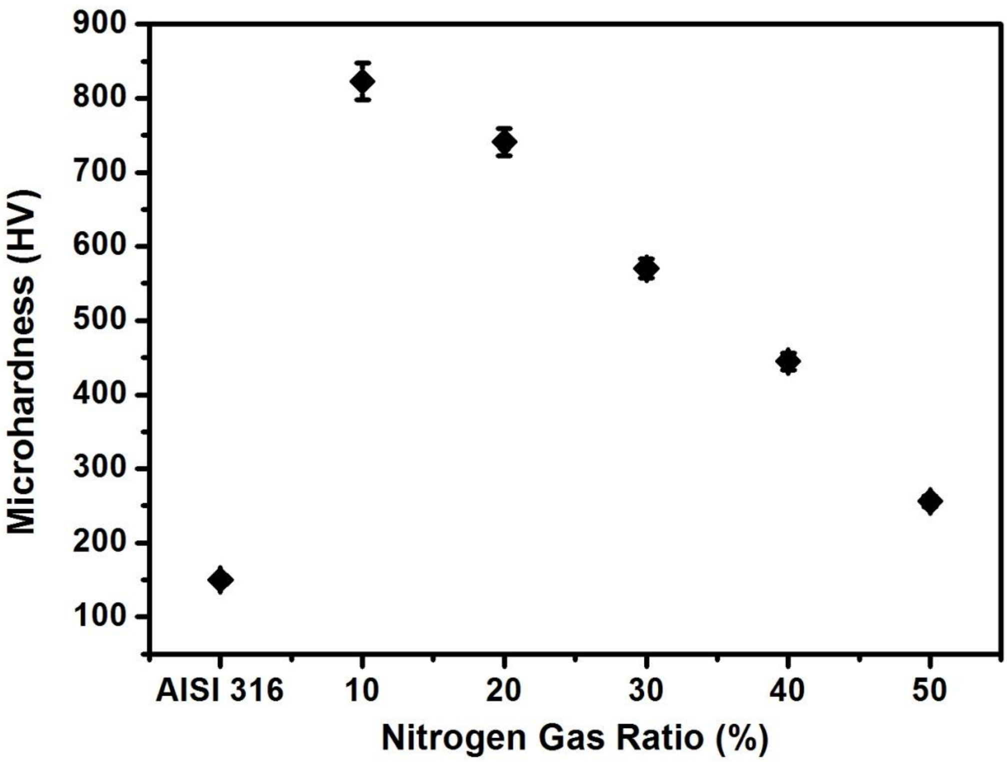

Fig. 6: Surface hardness of AISI 316 and coated substrates with TiAlN at different nitrogen gas percentage with respect to argon

3.3.2 Tribological properties

Figure 7 represented the average friction coefficient as a function of nitrogen gas ratio. It was discovered; all coated samples with TiAlN have lower average friction coefficient compared to the substrate. The reduction in friction coefficient is recognized to the crystal structure, chemical composition and high coating hardness [16]. The increase in the friction coefficient for samples deposited at 40 and 50 % nitrogen gas ratio is related to the worn out of the film. Otherwise, the increase in the film roughness at high nitrogen gas ratio may be added to the increase in friction coefficient. Figure 8 showed the optical micrographs of the wear tracks of the investigated samples. It was perceived; the wear track dimensions of the uncoated AISI 316 substrate are larger than that of TiAlN coatings. The sample coated at 10 % N_2 has lowest wear track due to the highest film thickness and microhardness. This validated to the enrichment in the wear resistance of TiAlN coatings in comparison with the uncoated substrate. Supplementary, the sample coated at nitrogen gas ratio of 10 % adhered well with the substrate (the tracks have sharp edge and there is flaking off for the coating). The samples coated at nitrogen gas ratios of 40 and 50 % have bad adherence with substrate where a flaking off for the films have been observed. Table 2 presented the wear track and the wear volume loss of the involved samples. The wear loss of TiAlN coating at 10 % nitrogen gas ratio is decreased by a factor of approximately 10^2 with respect to the AISI 316. It was perceived; the wear volume loss increased with increasing nitrogen gas ratio due to the worn out of the film species which contributed in increasing the wear volume loss.

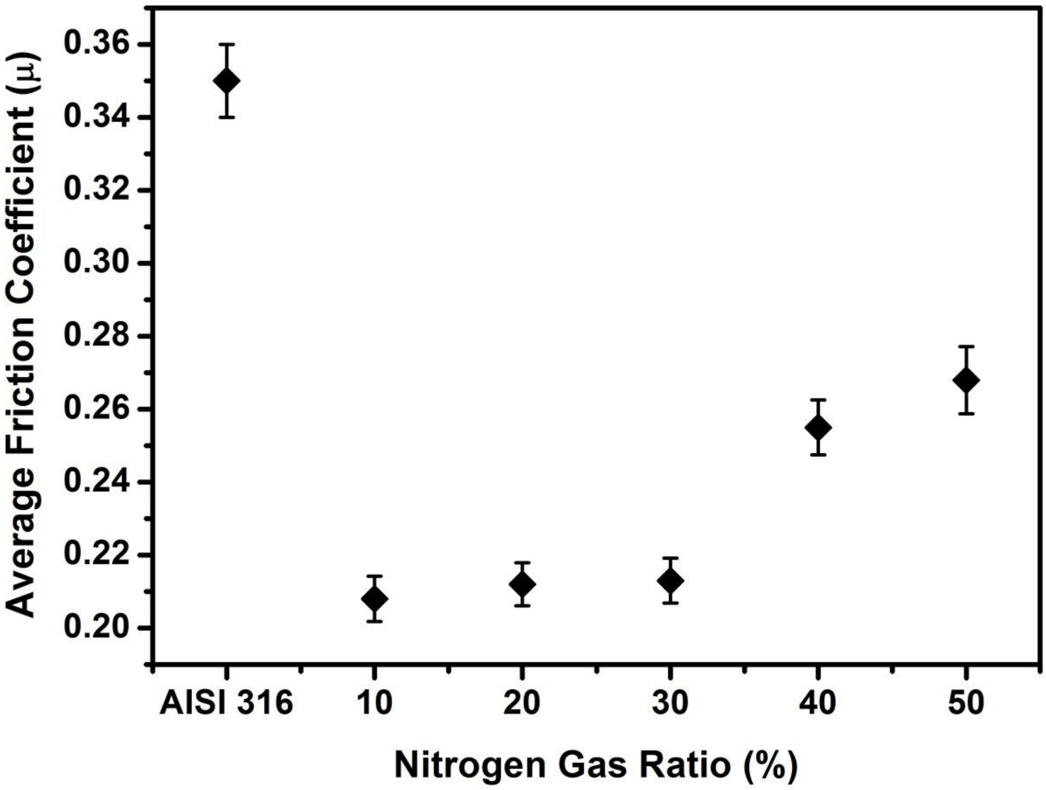

Fig. 7: The average friction coefficient of the examined samples at different nitrogen gas percentage with respect to argon

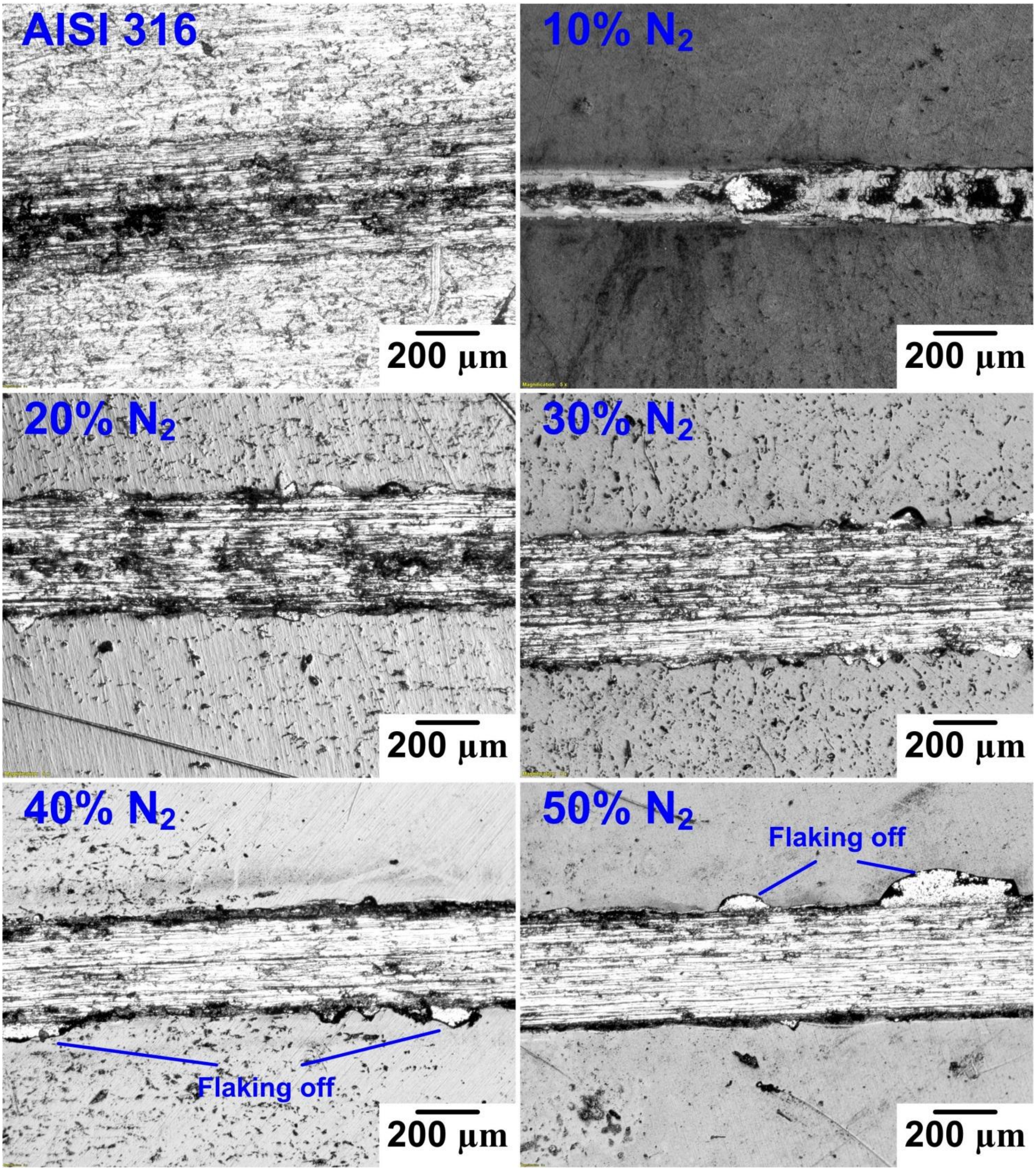

Fig. 8: Optical micrographs of wear tracks of TiAlN coatings at different nitrogen gas percentage with respect to argon

Table 2: The wear track width and the wear volume loss of the involved substrates

Sample	Track Width (μm)	Wear Volume Loss (μm^3)
AISI 316	445	$4.53X10^6$
10 % N2	180	$0.087X10^6$
20 % N2	329	$1.77X10^6$
30 % N2	373	$2.03X10^6$
40 % N2	386	$2.44X10^6$
50 % N2	420	$3.45X10^6$

3.4 Surface Roughness

The Ra parameter was acquired using a Form Talysurf 50 profilemeter. The uncoated AISI 316 substrate was ground and polished to give a preliminary surface roughness Ra of practically 0.054 μm. Figure 9 displays the average Ra value for the considered samples as a function of nitrogen gas ratio. It was observed; the Ra of TiAlN coating increased from 0.020 μm to 0.127 μm as the nitrogen gas ratio increased from 10 to 50 % respectively. The variation in Ra parameter from the uncoated to TiAlN coated substrates is authorized to the change in surface chemical composition and surface topography due to the deposition of TiAlN on the top surface. Moreover, the decrease in surface roughness at low nitrogen gas ratio range is recognized to the padding of surface irregularities with the depositing materials. Further, the increase in nitrogen gas ratio lead to the decrease in surface diffusivity of adatoms to substrate therefore; few nuclei can be initiated and grow to dome-shaped crystallites with voids in between [17] which in turn increase the surface roughness of the TiAlN coatings at high nitrogen gas ratio.

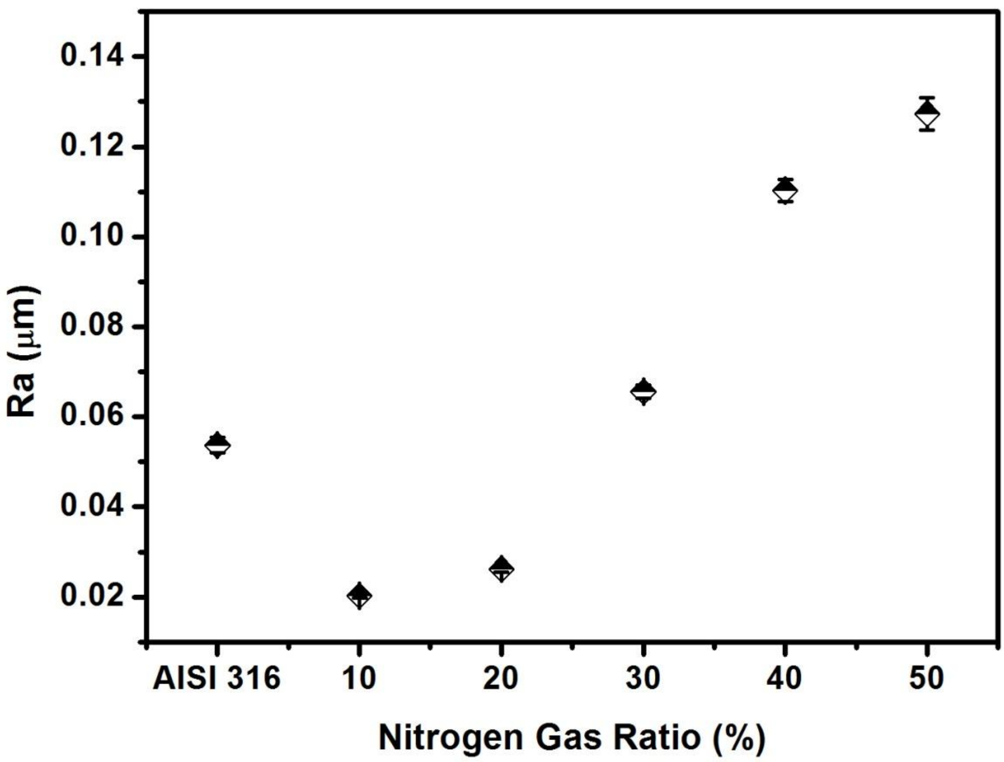

Fig. 9: The Ra of the uncoated and coated substrates with TiAlN at different nitrogen gas percentage with respect to argon

3.5 Corrosion Performance

Figure 10 displays the potentiodynamic polarization curves of the involved samples in ranger's solution. Moreover, the corrosion potential and current for all the examined samples are presented in Table 3. It was observed; the corrosion resistance were improved for all TiAlN coated substrates compared with uncoated one [18]. Moreover, the decrease in the corrosion current (Icorr) was witnessed for TiAlN coating deposited at low nitrogen gas ratio which reflected an enhancement in the corrosion resistance. Further, the uncoated sample showed stability in anodic current until potential equal to 400 mV then the current is sharply increased. All samples coated with TiAlN showed stability in anodic current at high potential compared with the uncoated one. Further, samples coated at high nitrogen gas ratio showed stability in anodic current at potential lower than the samples coated at low nitrogen gas ratio. This indicates that the passivation of the coated samples is broken down at higher potential than the uncoated one from one hand and the passivation of the coated samples at lower nitrogen flow ratios is broken down at higher potential than the samples coated at higher nitrogen gas ratios from the other hand. These observations reflected that the corrosion resistance of the samples coated at lower nitrogen gas ratios is better than the uncoated samples and the samples coated at higher nitrogen gas ratios. The increase in film thickness of TiAlN coatings resulted in enhancing the corrosion resistance [19]. The enhancement in corrosion resistance for TiAlN is credited to the formation of Al_2O_3 layer on the surface of the coatings which passivates the surface and averts further corrosion attack [20].

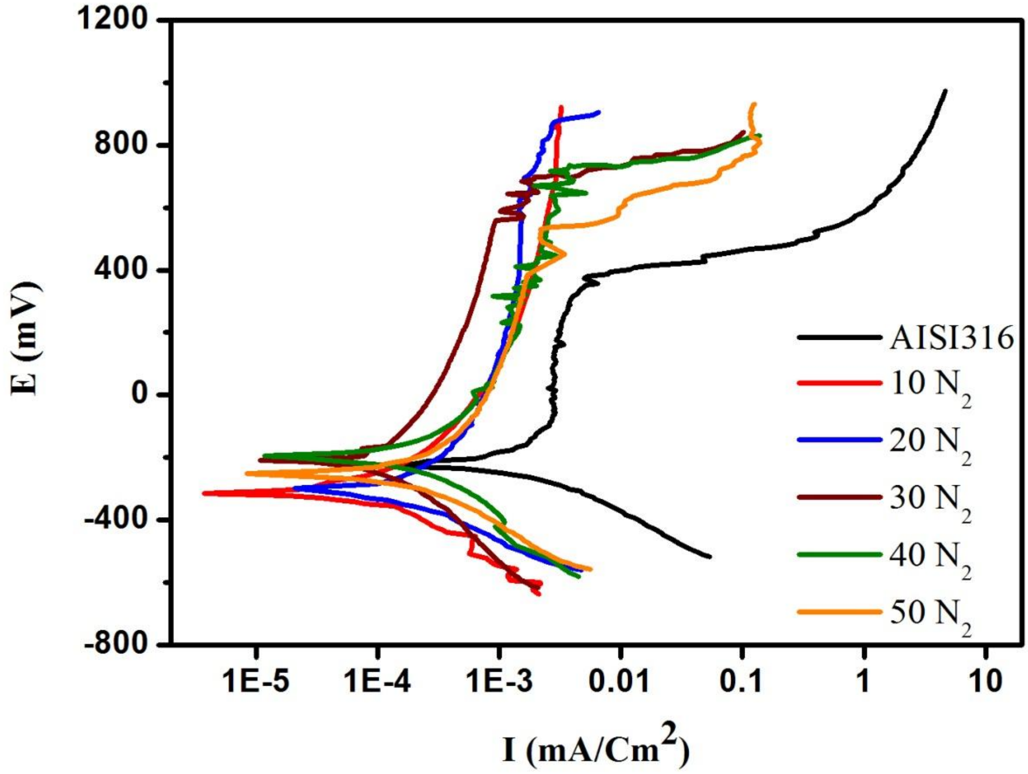

Fig. 10: The potentiodynamic polarization curves of the involved samples in Ringer's solution

Table 3: Corrosion data for AISI 316 and coated substrates with TiAlN at different nitrogen gas percentage in Ringer's solution.

Sample	I Corrosion (mA/Cm^2)	E Corrosion (mV)
AISI 316	0.0017499	-225.69
TiAlN (10% N_2)	0.0000901	-247.99
TiAlN (20% N_2)	0.0001416	-304.45
TiAlN (30% N_2)	0.0001381	-209.31
TiAlN (40% N_2)	0.0001948	-196.51
TiAlN (50% N_2)	0.0001981	-250.31

Conclusion

Worthy tribo-mechanical and electrochemical properties of TiAlN coatings deposited by Dc. Pulsed magnetron sputtering on AISI 316 substrates have been realized. It was found; the change in nitrogen gas ratio has a gigantic effect on the physico-chemical properties of the coatings. The hardness value increases to approximately 5-fold with respect to that of AISI 316 substrates. The wear rate decreased by a factor of 10^2 and the friction coefficient is decreased to nearly 2-times comparing with that of AISI 316 substrates. The formation of solid solution phase of TiAlN with desirable physic-chemical properties and with high adhesion between the coating and the substrate are responsible for this improvement in the properties. It was concluded;

1- The coatings prepared at low nitrogen gas ratio have precious mechanical and electrochemical properties than the coatings prepared at high nitrogen gas ratio

2- Dc. Pulsed magnetron sputtering is a robust method for preparing thin films that can be used in many engineering applications.

Reference

[1] S. Paldey, S.C. Deevi, Mater. Sci. Eng., A 342 (2003) 58.

[2] W.D. Mu¨ nz, L.A. Donohue, P.Eh. Hovsepian, Surf. Coat. Technol. 125 (2000) 269.

[3] F. Weber, F. Fontaine, M. Scheib, W. Bock, Surf. Coat. Technol. 177– 178 (2004) 227.

[4] H.G. Prengel, A.T. Santhanam, R.M. Penich, P.C. Jindal, K.H. Wendt, Surf. Coat. Technol. 94– 95 (1997) 597.

[5] P.J. Kelly, R.D. Arnell, Vacuum 56 (2000) 159–172.

[6] Schiller S, Goedicke K, Reschke J, Kircho! V, Schneider S, Milde F, Surf Coat Technol 61 (1993) 331–337.

[7] Scherer M, Schmitt J, Latz R, Schanz M, J Vac Sci Technol A 10 (1992) 1772.

[8] F. M. El-Hossary, A. M. Abd El-Rahman, M. Raaif, Shuxin Qu, Junsheng Zhao, Manfred F. Maitz, M. Abo EL-Kassem, Applied Physics A 124 (2017) 42.

[9] ASTM standard E384, 2011, ASTM International, West Conshohocken, PA 19428-2959, United States, DOI: 10.1520/E0384-11.

[10] J.V. Ramana, Sanjiv Kumar, Christopher David, V Raju, Materials Letters 58 (2004) 2553– 2558.

[11] L. Chen, M. Moser, Y. Du, P.H. Mayrhofer, Thin Solid Films 517 (2009) 6635–6641.

[12] Yongqiang Wei, Chunzhi Gong, Applied Surface Science 257 (2011) 7881–7886

[13] S. Chinsakolthanakorn, A. Buranawong, N. Witit-anun, S. Chaiyakun, P. Limsuwan, Procedia Engineering 32 (2012) 571 – 576.

[14] Yan Pei, Deng Jianxin, Wu Ze, Li Shipeng, Xing Youqiang, Zhao Jun, Int. Journal of Refractory Metals and Hard Materials 35 (2012) 213–220.

[15] Wenji Zhao, Fanghua Mei, Yunshan Dong, Geyang Li, Journal of Materials Processing Technology 176 (2006) 179–182.

[16] L. Ipaz, J.C. Caicedo, J. Esteve, F. J. Espinoza-Beltran, G. Zambrano, Applied Surface Science, 258 (2012) 3805-3814.

[17] S. PalDey, S.C. Deevi, Materials Science and Engineering A342 (2003) 58-79.

[18] Martin Fenker, Martin Balzer, Herbert Kappl, Surface and Coating Technology 257 (2014) 182-205.

[19] J. Aromaa, H. Ronkainen, A. Mahiout, S.-P. Hannula, Surface and Coating Technology 49 (1991) 353-358.

[20] L. Cunha, M. Andritschky, L. Rebouta, K. Pischow, Surface and Coating Technology 116-119 (1999) 1152-1160.